Materials Science & Engineering C 105 (2019) 110043

Contents lists available at ScienceDirect

Materials Science & Engineering C

journal homepage: www.elsevier.com/locate/msec

^{177}Lu-Bombesin-PLGA (paclitaxel): A targeted controlled-release nanomedicine for bimodal therapy of breast cancer

Brenda Gibbens-Bandala[a,b], Enrique Morales-Avila[b], Guillermina Ferro-Flores[a], Clara Santos-Cuevas[a], Laura Meléndez-Alafort[c], Maydelid Trujillo-Nolasco[a,b], Blanca Ocampo-García[a,*]

[a] Departamento de Materiales Radiactivos, Instituto Nacional de Investigaciones Nucleares, Carretera México-Toluca S/N, Ocoyoacac, Estado de México 52750, Mexico
[b] Facultad de Química, Universidad Autónoma del Estado de México, Paseo Tollocan S/N, Toluca, Estado de México 50180, Mexico
[c] Veneto Institute of Oncology IOV-IRCCS, Via Gattamelata 64, Padova 35128, Italy

ARTICLE INFO

Keywords:
Radiotherapy
Targeted therapy
Smart nanoparticles
Drug delivery
Cancer
Concomitant cancer treatment

ABSTRACT

The gastrin-releasing peptide receptor (GRPr) is overexpressed in > 75% of breast cancers. ^{177}Lu-Bombesin (^{177}Lu-BN) has demonstrated the ability to target GRPr and facilitate efficient delivery of therapeutic radiation doses to malignant cells. Poly(D,L-lactide-co-glycolide) acid (PLGA) nanoparticles can work as smart drug controlled-release systems activated through pH changes. Considering that paclitaxel (PTX) is a first-line drug for cancer treatment, this work aimed to synthesize and chemically characterize a novel polymeric PTX-loaded nanosystem with grafted ^{177}Lu-BN and to evaluate its performance as a targeted controlled-release nanomedicine for concomitant radiotherapy and chemotherapy of breast cancer.

PLGA(PTX) nanoparticles were synthesized using the single emulsification-solvent evaporation method with PVA as a stabilizer in the presence of PTX. Thereafter, the activation of PLGA carboxylic groups for BN attachment through the Lys^1-amine group was performed. Results of the chemical characterization by FT-IR, DLS, HPLC and SEM/TEM demonstrated the successful synthesis of BN-PLGA(PTX) with a hydrodynamic diameter of 163.54 ± 33.25 nm. The entrapment efficiency of paclitaxel was 92.8 ± 3.6%. The nanosystem showed an adequate controlled release of the anticancer drug, which increased significantly due to the pH change from neutral (pH = 7.4) to acidic conditions (pH = 5.3). After labeling with ^{177}Lu and purification by ultrafiltration, ^{177}Lu-BN-PLGA(PTX) was obtained with a radiochemical purity of 99 ± 1%.

In vitro and *in vivo* studies using MDA-MB-231 breast cancer cells (GRPr-positive) demonstrated a ^{177}Lu-BN-PLGA(PTX) specific uptake and a significantly higher cytotoxic effect for the radiolabeled nanosystem than the unlabeled BN-PLGA(PTX) nanoparticles. Using a pulmonary micrometastasis MDA-MB-231 model, the added value of ^{177}Lu-BN-PLGA(PTX) for tumor imaging was confirmed. The ^{177}Lu-BN-PLGA(PTX) nanomedicine is suitable as a targeted paclitaxel delivery system with concomitant radiotherapeutic effect for the treatment of GRPr-positive breast cancer.

1. Introduction

Recently, nanoradiopharmaceuticals have received more attention as suitable approaches for imaging and/or therapy for several cancer types. Nanoparticles (NPs) offer useful platforms for the design of more effective drug delivery systems. Moreover, NPs can be functionalized to allow target-specific recognition towards receptors overexpressed in malignant tissues. Particularly, polymeric nanoparticles have generated special interest in the field of cancer treatment due to their ability to encapsulate drugs and release them in a controlled manner [1]. Poly lactic-co-glycolic acid (PLGA) is approved for human use as a smart nanosystem for drug delivery due to its response to pH changes, biocompatibility and biodegradability [2,3]. Usually, a therapeutic agent is dispersed throughout the polymeric matrix or can be encapsulated in the hydrophobic nanoparticle core.

Paclitaxel (PTX) has become a first-line drug for the treatment of solid cancers. However, its use is hampered by its toxicity, poor bioavailability and severe side effects. Hence, the drug has been used as a

* Corresponding author at: Departamento de Materiales Radiactivos, Instituto Nacional de Investigaciones Nucleares, Carretera México-Toluca S/N, La Marquesa, Ocoyoacac, Estado de México C.P. 52750, Mexico.
E-mail address: blanca.ocampo@inin.gob.mx (B. Ocampo-García).

https://doi.org/10.1016/j.msec.2019.110043
Received 22 March 2019; Received in revised form 26 June 2019; Accepted 31 July 2019
Available online 01 August 2019
0928-4931/

model to evaluate and optimize drug delivery systems based on nanoparticles [4].

Bombesin (BN) is a homolog to the mammalian gastrin-releasing peptide (GRP) and has demonstrated high sensitivity to detect the GRP receptor (GRPr) in breast cancer [5]. Recently, a study of 1432 tumor patients revealed that GRPr is overexpressed in 75.8% of several phenotypes of breast cancer and was also found in metastatic lymph nodes in 94.6% of cases [6]. A variety of BN derivatives radiolabeled with different radionuclides have been widely studied as targeting ligands for diagnosis and/or therapy of GRPr-positive tumors [2,7]. Moreover, BN can properly be attached to the surface of a nanoparticle to enhance its affinity towards a desired molecular target [8–10]. Polymeric nanoparticles functionalized with BN have been proposed as suitable drug delivery systems [11,12].

Lutetium-177 (^{177}Lu, half-life of 6.6 days) is a theranostic beta-emitter (E_{max} of 498.3 keV), a feature that enables it to produce cytotoxicity towards tumors or metastatic lesions (particle range in tissue around 2 mm), and a gamma-emitter (E_{max} = 208 keV), which makes it useful for imaging [5]. ^{177}Lu-BN derivatives have been tested on patients with prostate cancer overexpressing GRPr and represent a useful tool for diagnostic imaging and targeted radiotherapy [5,13].

Considering that paclitaxel (PTX) is a first-line drug for the treatment of solid cancers and taking advantage of the therapeutic effect of ^{177}Lu-Bombesin, this work aimed to prepare and evaluate a novel ^{177}Lu-labeled PTX-loaded nanocarrier grafted to Lys^{1}Lys^3(^{177}Lu-DOTA) Bombesin in breast cancer cells as a potential combined therapy system for breast cancer.

2. Materials and methods

2.1. Materials

Paclitaxel (PTX), Poly(D,L-lactide-co-glycolide) acid (50:50 M_W 24,000–38,000 g/mol) and Poly(vinyl alcohol) (PVA; Mowiol®4-88) were purchased from Sigma-Aldrich (St. Louis Missouri, USA). The Lys^{1}Lys^3(DOTA)-Bombesin(1-14) peptide [Bombesin, BN] was obtained from Bachem (Product 4097020) laboratory (Graz, Austria); lutetium-177 (^{177}Lu), as lutetium chloride ($^{177}LuCl_3$), was supplied by ITG (Germany); dimethylformamide (DMF), *N,N*-diisopropylethylamine (DIPEA), 2-(1H-7-azabenzotriazol-1-yl)-1.1.3.3-tetramethyluronium-hexafluorophosphate (HATU) and all other reagents were analytical grade. The XTT kit was obtained from Roche Diagnostics (Indianapolis, IN. USA) and MDA-MB-231 cell line was obtained from ATCC (Atlanta, GA, USA).

2.2. Preparation of PLGA nanoparticles

PLGA nanoparticles (hereafter denoted PLGA) were prepared using the single emulsification-solvent evaporation method, employing PVA as stabilizer [14]. Briefly, an organic solution of the Poly(D,L-lactide-co-glycolide) acid polymer (15 mg/mL in acetone) and methanol (1.32 mL) was mixed and immediately added drop-wise onto a 0.25% PVA solution (7.29 mL) under ultra-sonication in an ice bath. After 10 min, acetone/methanol were removed using a rotary vacuum evaporator (65 °C, 40 rpm, 20 min). The obtained nano-suspension was filtered and washed with injectable-grade water by ultracentrifugation (MWCO 30 kDa, 2500*g*, 30 min) and the pellet was freeze-dried for 24 h.

2.3. Preparation of paclitaxel-loaded nanoparticles

To prepare paclitaxel-loaded nanoparticles [PLGA(PTX)], the PLGA polymer (15 mg/mL in acetone) and 1 mg of paclitaxel in acetone solution were placed in magnetic stirring for 30 min. Posteriorly, methanol (1.32 mL) was added. Then, the procedure mentioned above for PLGA synthesis was applied (Fig. 1).

The non-incorporated drug was removed by ultracentrifugation (MWCO 30 kDa, 2500*g*, 30 min), and the purified nano-suspension obtained was freeze-dried and stored for posterior use.

2.4. Bioconjugation of bombesin to polymeric nanoparticles

Lys^{1}Lys^3(DOTA)-Bombesin was conjugated to PLGA and PLGA(PTX) NPs to prepare BN-PLGA or BN-PLGA(PTX) systems. Briefly, lyophilized PLGA or PLGA(PTX) NPs (5 mg) were dissolved in 50 μL of water and 100 μL of DMF; 100 μL of DIPEA solution (10 μL of DIPEA in 300 μL of DMF) and the carboxylate-activating agent HATU (10 mg in 100 μL of DMF) were added. The mix was then exposed to sonication for 15 min. Lys^{1}Lys^3(DOTA)-BN (1 mg/100 μL in DMF) was afterwards added, and the mixture was incubated under slow stirring for 2 h at room temperature (Fig. 1). The obtained nano-suspensions, BN-PLGA or BN-PLGA(PTX), were purified by ultracentrifugation, as previously described.

2.5. Radiolabeling

BN-PLGA and BN-PLGA(PTX) NPs were radiolabeled through the DOTA bifunctional chelator on the Lys^{1}Lys^3(DOTA)-Bombesin structure with ^{177}Lu (Fig. 1). Radiolabeling was carried out by adding $^{177}LuCl_3$ solution (10 μL, 148 MBq) to the BN-PLGA or BN-PLGA(PTX) (500 μg in 40 μL of 0.25 M acetate buffer, pH 7). Each mixture was then heated at 37 °C for 3 h. Nanoparticles were purified by ultracentrifugation (MWCO 30 kDa, 2500*g*, 20 min). Both fractions (filtered and unfiltered) were measured in an activimeter (Capintec, USA) to calculate the radiolabeling yield of ^{177}Lu-BN-PLGA and ^{177}Lu-BN-PLGA(PTX). To evaluate the radiochemical purity, ITLC-SG strips (Pall Corporation) were used as stationary phase and NaCl 0.9%/0.02 M HCl, as mobile phases. Free lutetium was identified at the solvent front (Rf = 1.0).

2.6. Physicochemical characterization

2.6.1. Hydrodynamic diameter and zeta potential

Adequate aqueous dilutions of the nanosystems [PLGA, PLGA(PTX), BN-PLGA, BN-PLGA(PTX)] were used to measure particle size and zeta potential through Dynamic Light Scattering (DLS) using a nanoparticle size analyzer (Nanotrac Wave, Model MN401, Microtract, FL, USA). The analysis was performed at a wavelength of 657 nm at 20 °C, current of 15.79 mA, electric field of 14.35 V/cm and sampling time of 128 μs, in triplicate.

2.6.2. Scanning electron microscopy (SEM) and transmission electron microscopy (TEM)

Morphology of the obtained systems was examined through SEM. A drop of each sample was placed on a metal slab, dried and coated with a gold layer (Denton Vacuum DESK IV sputtering system, Moorestown, NJ). The coated samples were scanned using an electron acceleration voltage of 20–25 keV (JEOL JSM-5900 Low Vacuum, USA).

Additionally, systems were analyzed through TEM in a JEOL JEM 2010 HT microscope operating at 200 kV to observe the relative size and morphology. Samples were prepared for analysis by evaporating a drop of aqueous product on a carbon-coated TEM copper grid.

2.6.3. Infrared spectroscopy

The FT-IR measurements were performed on a PerkinElmer System 2000 spectrometer with an attenuated total reflection (ATR) platform (Pike Technologies). The spectra were obtained from 50 scans at a 0.4 cm^{-1} resolution, from 400 to 4000 cm^{-1}.

2.7. Entrapment efficiency

Drug analysis was carried out through high-performance liquid chromatography (HPLC) using a reverse phase C18 column

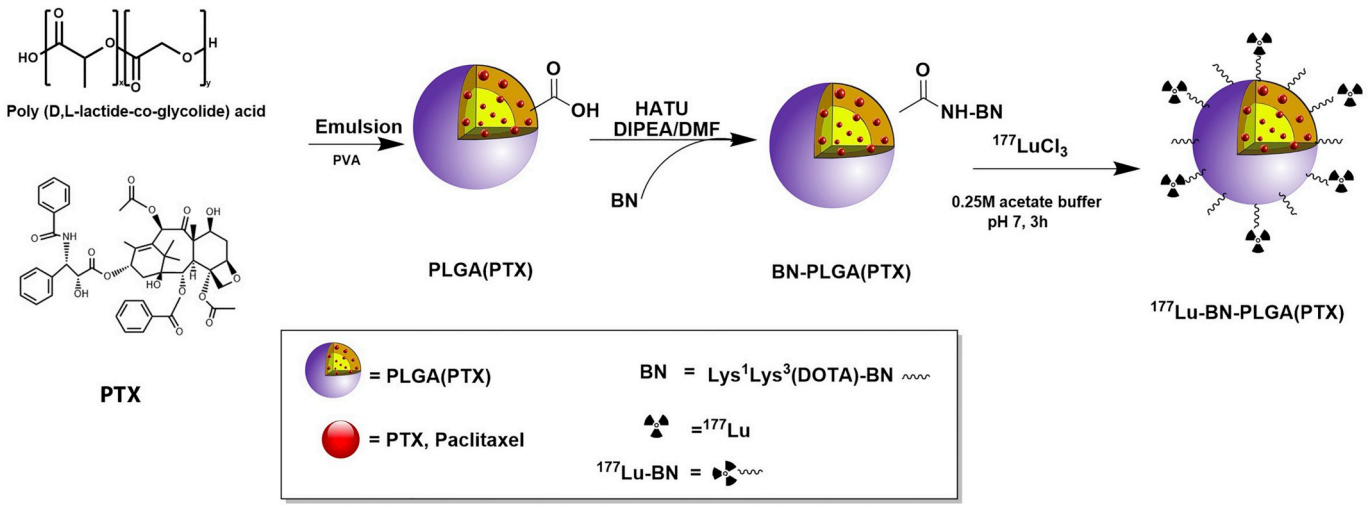

Fig. 1. Schematic representation of PLGA(PTX), BN-PLGA(PTX) and ^{177}Lu-BN-PLGA(PTX) nanosystems.

(μBondapak®, 10 μm 125A°, 3.9 × 150 mm) as the stationary phase and acetonitrile:water (60:40 v/v) as the mobile phase. Separation was carried out at a flow rate of 1 mL/min, with a run time of 5 min for each sample. PTX was measured at 227 nm on a Waters Empower system using a PTX calibration curve (r^2 of 0.997, 6.0–300.0 μg/mL). The experiments were conducted in triplicate.

The encapsulation efficiency (%EE) and drug loading (%DL) were evaluated through HPLC analysis. The concentration of non-encapsulated PTX in the filtered solution was obtained from the ultracentrifugation process (MWCO 30 kDa, 2500*g*, 20 min). These parameters, expressed as a percentage, were determined as follows:

$$\%EE = \left(\frac{Mass\ of\ PTX\ in\ nanoparticles}{Initial\ Mass\ of\ PTX}\right) \times 100 \quad (1)$$

$$\%DL = \left(\frac{Mass\ of\ PTX\ in\ nanoparticles}{Mass\ of\ nanoparticles}\right) \times 100 \quad (2)$$

2.8. In vitro PTX release

For the *in vitro* drug release studies, a solution of phosphate-buffered saline (PBS) containing 0.05% Tween-20, at pH 7.4 or pH 5.3, simulating physiological pH or tumor microenvironment, respectively, was used. Briefly, 10 mg of PLGA(PTX) were dispersed in 1 mL of release medium and placed in a dialysis membrane (MWCO 30 kDa). The dialysis bag was closed and immersed into a flask containing PBS (10 mL) at 37 °C and stirred at 110 rpm. At specified time points, an aliquot of 0.2 mL of the medium was collected and replaced with fresh PBS. Released PTX was measured through HPLC based on the previously described methodology [15].

2.9. Bombesin conjugation efficiency

Conjugation efficiency was determined by measuring free BN in the filtered solution after ultracentrifugation. The reverse-phase HPLC method was carried out using a C18 column (μBondapak® C18 10 μm 125A°, 3.9 × 300 mm) as a stationary phase and a gradient of water/acetonitrile containing 0.1% TFA from 95/5 (v/v) to 20/80 (v/v) as the mobile phase. Separation was carried out at a flow rate of 1 mL/min and a run time of 30 min. A BN standard curve (r^2 = 0.999, 0.07–2.2 mg/mL) was used in this analysis.

2.10. In vitro studies

2.10.1. Cell lines

MDA-MB-231 human breast cancer cells (GRPr-positive) [5,16,17] were originally obtained from the American Type Culture Collection (USA). The cells were routinely grown at 37 °C, with 5% CO_2 atmosphere and 85% humidity in RPMI medium supplemented with 10% newborn calf serum and antibiotics (100 μg/mL streptomycin, 100 U/mL penicillin).

2.10.2. In vitro binding assay and non-specific binding

MDA-MB-231cells were harvested through trypsinization and seeded in 24-well culture plates (1 × 10^5 cells/well, 0.5 mL). After 24 h, the medium was removed and the cells were incubated with adequate treatment dilution (^{177}Lu-BN-PLGA(PTX) or ^{177}Lu-BN, equivalent to 50 kBq per well) for 45 min at 37 °C. Each well was then rinsed twice with PBS. To displace the membrane-bound radiopharmaceutical fraction, cells were incubated twice (5 min, 37 °C) with 500 μL of 20 mM Gly/HCl, and the activity of the total withdrawn volume was transferred to counting tubes. The cells were then incubated twice with 500 μL of a 1 M NaOH solution (5 min, 37 °C); this fraction (cytoplasm and nucleus) represented nanosystem internalization. The total volume was transferred to counting tubes. Radioactivity in each tube was measured in a gamma NaI(Tl) detector (NML Inc., USA). An aliquot with the initial activity was measured as the radioactivity standard in each treatment. The uptake percentage was calculated. Non-specific binding (cells with blocked receptors) was determined in parallel, in the presence of 5.7 μM Lys^{1}Lys^3(DOTA)-BN with 10 min of pre-incubation.

2.10.3. Cytotoxicity studies

To compare the cytotoxic effect produced by ^{177}Lu-BN-PLGA(PTX), different treatments (PLGA, PLGA(PTX), BN-PLGA, ^{177}Lu-BN-PLGA(PTX), PTX, ^{177}Lu-BN) were evaluated in MDA-MB-231 cells, mainly to compare the PTX contribution since the effect produced by the β-emission of ^{177}Lu is well-documented. A sublethal dose was used to determine differences among treatments without the cell-killing effect. The concentration of nanosystems for radiolabeling was calculated in terms of PTX content and adjusted to 1.5 μM to use one-tenth of the lethal dose based on previous reports (breast cancer cells IC_{50} = 15 μM [18]).

The cytotoxic activity was measured using a Cell Proliferation Assay (XTT) kit, according to the manufacturer's protocol (Roche Diagnostics GmbH, Mannheim, Germany). Cells were seeded in a 96-well microtiter plate (1 × 10^4 cells/well) and incubated overnight to allow cell

attachment. Then, the medium was removed and 50 μL of each treatment and 200 μL of RPMI medium were placed in each well. The viability was evaluated after removing the medium at 72 h (37 °C, 5% CO_2 and 85% humidity).

2.10.4. Study of the synergistic therapeutic effect

To evaluate the chemotherapeutic (PTX) and radiotherapeutic (^{177}Lu) synergistic effect of the radiolabeled nanosystem on cell viability, 1×10^4 cells/well were exposed to ^{177}Lu-BN-PLGA(PTX) or unlabeled (BN-PLGA(PTX) nanosystems (30 μM in terms of PTX content). The viability was evaluated through the XTT protocol at 24, 48 and 72 h.

2.10.5. Estimation of radiation-absorbed doses to the MDA-MB-231cell nucleus

To estimate the radiation-absorbed doses to the MDA-MB-231 cell nucleus, the following equation was used:

$$D_{N \leftarrow Source} = (N_M \times DF_{N \leftarrow M}) + (N_C \times DF_{N \leftarrow C}) \quad (3)$$

where $D_{N \leftarrow Source}$ represents the mean absorbed dose to the nucleus from source regions (membrane and cytoplasm) and N_M and N_C are the total number of nuclear disintegrations that occurred in the membrane and cytoplasm. $DF_{N \leftarrow M}$ and $DF_{N \leftarrow C}$ denote the dose factors specific for ^{177}Lu, from membrane and cytoplasm regions to the nucleus configuration. The dose factor geometries were obtained from the S values reported by Goddu and Budinger (cell radius = 10 μm, nucleus radius = 5 μm) [19].

2.10.6. Hemocompatibility

For medical devices projected for direct or indirect blood exposure, hemocompatibility studies are required [20]. In this work, the potential of the nanosystems to disrupt red blood cells (RBC) was assessed by the hemolytic assay.

The hemolytic assay was performed in agreement with the standard ISO 10 993-4. Briefly, 200 μL of each treatment ($n = 3$) was placed in contact with 5% human RBC. Trials were immediately incubated at 37 °C for 1 h with negative (isotonic saline) and positive controls (distilled water). Optical density (OD) produced in each treatment was measured at 415 nm (Lambda Bio, Perkin Elmer, USA). The percentage of hemolysis was calculated according to Eq. 4.

$$\%Hemolysis = \frac{OD_{test} - OD_{negative}}{OD_{positive} - OD_{negative}} \times 10 \quad (4)$$

2.11. In vivo studies

In vivo studies in mice were carried out according to the Official Mexican Norm 062-ZOO-1999. Athymic female mice (6–7 weeks of age) were identified and transferred inside plastic cases, kept at a constant temperature, humidity, 12:12 light:dark periods and fed *ad libitum*.

2.11.1. Tumor induction

a) Tumor model for single-photon emission computed tomography (SPECT/CT) imaging and biodistribution studies

Athimic female mice received an intravenous (caudal vein, for pulmonary tumor model) or subcutaneous (upper back, for subcutaneous tumor model) inoculation of 1×10^6 MDA-MB-231 cancer cells suspended in 0.1 mL of phosphate-buffered saline, and 2 weeks after inoculation the animals were used for the imaging or biodistribution studies, respectively.

b) Tumor model for FDG-PET/CT (^{18}F-deoxyglucose-positron emission tomography/computed tomography) and SUV (standard uptake value) calculation.

To assess the extent of tumoral progression under exposure to different treatments, breast tumors (MDA-MB-231 cells, 1×10^6 in PBS) were subcutaneously inoculated on the upper back of 16 female athymic mice (5–6 weeks of age) and the inoculation site was observed for the development of a tumor. Mice survival and size tumor were monitored for 12 days.

2.11.2. Micro SPECT-CT imaging

To verify the *in vivo* nano-radiosystem retention in induced pulmonary tumors, SPECT-CT images were acquired using a micro-SPECT/CT scanner (Albira, ONCOVISION; Gem Imaging S.A., Valencia, Spain) 72 h after intravenous ^{177}Lu-BN-PLGA(PTX) administration (5 MBq in 0.1 mL PBS). Mice under 2% isoflurane anesthesia were placed in the prone position and imaging was performed. The micro-SPECT field of view was 60 mm; a symmetric 20% window was set at 140 keV, and pinhole collimators were used to acquire a three-dimensional SPECT image with a total of 64 projections of 30 s each over 360°. The image dataset was then reconstructed using the ordered-subset expectation maximization algorithm with the standard mode parameter, as provided by the manufacturer. CT parameters were 35 kV sure voltage, 700 μA current and 600 micro-CT projections.

2.11.3. Biodistribution

The subcutaneous tumor model animals received 5 MBq in 0.1 mL of ^{177}Lu-BN-PLGA(PTX). Seventy-two hours after injection, the mice were euthanized and the blood and main organs were removed and placed into pre-weighed plastic test tubes. The radioactivity was measured in a well-type scintillation Na(Tl) detector along with two aliquots of standards (representing 100% of injected activity) and expressed as percentages of the injected dose per gram (%ID/g) or per organ (%ID/organ).

2.11.4. FDG-PET/CT imaging

To assess the tumoral progression (Section 2.11.1), the female mice with MDA-MB-231 tumors were randomly separated into 4 groups. The mean volume of the tumors was 0.119 ± 0.035 cm^3, calculated as $V = \pi/6 * L * a^2$. The length (L) and width (a) were measured with Vernier calipers [21]. Mice were anesthetized with isofluorane 2% and administered intratumorally with each treatment as follows: a) 3 MBq of ^{177}Lu-BN-PLGA(PTX), b) 3 MBq of ^{177}Lu-BN-PLGA and the equivalent mass of c) PLGA(PTX) or d) PLGA as the control.

After 8 days of treatment, images were acquired on a micro-PET/CT scanner (Albira, ONCOVISION, Spain) and the tumor metabolic activity was measured through the Standardized Uptake Value (SUV) of ^{18}F-Deoxyglucose (FDG). The mice were administered with 70–100 μL (3–4 MBq) of FDG on the tail vein under anesthesia. After 1 h, whole body images were acquired in a micro-PET/CT, and the Standard Uptake Value (SUV) was calculated using PMOD Data Analysis software.

Finally, the mice were euthanized since the control tumor size was higher than 1.83 mm^3.

2.11.5. Tumor radiation absorbed dose estimation

The radiation-absorbed dose (the energy deposited by ionizing radiation per unit of mass expressed in Gy) of ^{177}Lu-BN-PLGA(PTX) and ^{177}Lu-BN-PLGA to tumor was calculated according to the following expressions:

$$N_{tumor} = \int_{t1}^{t2} A_h dt = A_0 \int_{0\,d}^{8\,d} e^{-\lambda t} = \frac{A_0}{\lambda}(1 - e^{-\lambda t}) \quad (5)$$

$$\overline{D}_{tumor \leftarrow tumor} = N_{tumor} DF_{tumor \leftarrow tumor} \quad (6)$$

where N = total number of disintegration in the tumor, $t_1 = 0$ day and $t_2 = 8$ day post-treatment, $\lambda = \ln 2/t_{1/2}$ or (ln2/6.7d), A_0 = initial administered Lu-177 activity (Bq), $\overline{D}_{tumor \leftarrow tumor}$ = mean absorbed dose to tumor from tumor, and DF is the dose factor for Lu-177.

The N value was introduced to Organ Level Internal Dose Assessment (OLINDA) code, (which provides conversion factors (DF)) to estimate the radiation-absorbed dose ($\overline{D}_{tumor \leftarrow tumor}$) delivered by Lu-177 administered with each treatment.

2.12. Statistical analysis

Differences in cell uptake between unblocked and blocked receptors were evaluated with the Student *t*-test. The cytotoxicity results were estimated by a two-sided ANOVA using OriginLab and GraphPrisma software, setting the statistical significance at $p < 0.05$.

3. Results and discussion

The application of polymeric nanoparticles for PTX release, GRPr targeting and targeted radiotherapy with ^{177}Lu has been studied in this research to achieve a dual therapeutic effect on MDA-MB-231 breast cancer cells.

3.1. Preparation of PLGA and PLGA(PTX) nanoparticles

In this research, minor modifications in the emulsion-solvent method [14] allowed us to obtain both the free-drug PLGA and paclitaxel-loaded PLGA nanoparticles. The hydrophobic hydrocarbon chains from the lactide moieties in PLGA enabled the interaction with hydrophobic PTX, allowing thermodynamic folding and the consequent nanoparticle formation [3].

Scanning Electron Microscopy and Transmission Electron Microscopy micrographs (Fig.2) showed that the designed nanosystems presented a well-shaped spherical form. The morphology was not modified by PTX incorporation or the grafted BN. All nanoparticle systems showed a hydrodynamic diameter < 200 nm (by DLS) and a monomodal distribution. A narrow polydispersity was observed for PLGA and PLGA(PTX) systems (Table 1). However, the PDI increased as a result of functionalization with BN (0.2896 and 0.2987). In general, a PDI smaller than 0.2 is considered as a narrow-size distribution [22]. Specifically, the size range was 104 nm to 201 nm for PLGA and 109 nm to 213 nm for PLGA(PTX), without significant differences ($p < 0.05$).

Table 1
Physicochemical characterization of nanoparticles.

Nanoparticle	Size (nm)	Polydispersity index (PDI)	Z potential (mV)
PLGA	152.90 ± 48.56	0.1977	−18.9
PLGA(PTX)	161.23 ± 52.27	0.1914	−19.0
BN-PLGA	156.19 ± 54.18	0.2896	−11.0
BN-PLGA(PTX)	163.54 ± 33.25	0.2987	−12.3

Negative zeta potential of PLGA nanoparticles (−18.9 mV) is attributed to the carboxylate groups on the nanoparticle surface. In PLGA(PTX), the Z potential remained unchanged in charge, which could mean that the paclitaxel remained entrapped in the nanoparticles, in agreement with the results of chemical characterization.

3.2. Conjugation of bombesin to PLGA or PLGA(PTX)

Bombesin was conjugated to the PLGA or PLGA(PTX) by the coupling peptide reaction, using HATU as the activator molecule. The attachment of BN onto the nanoparticle surface did not affect the translational diffusion coefficient, which can be understood as the maintenance in equivalent hydrodynamic diameter, keeping apparent nanoparticle sizes. However, the zeta potential showed a significant decrease from −18.9 mV to -11 mV in BN-PLGA and from −19.0 mV to −12.3 mV in BN-PLGA(PTX). The reduction in Z potential values suggests that the peptide interaction and arrangement on the nanoparticle surface originate changes in the electrostatic environment surrounding the nanoparticle. The positive amine, amide bonds and neutral hydrocarbon chains of Lys^{1}Lys^3(DOTA)-BN could contribute to the reduction

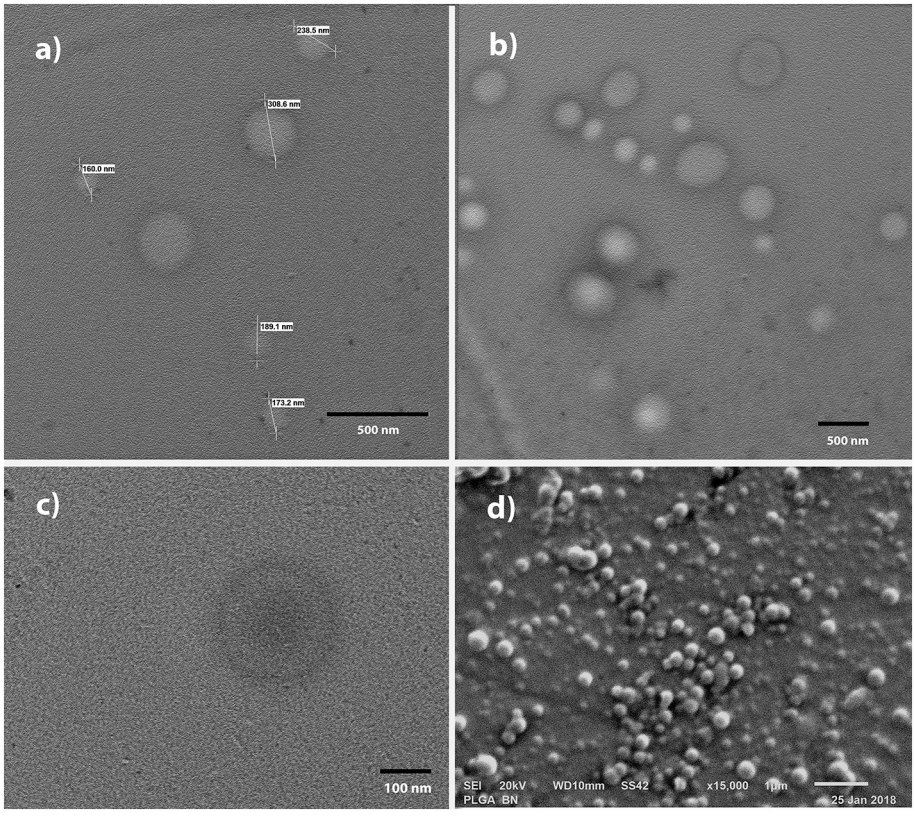

Fig. 2. Representative TEM micrograph of a) PLGA, b) PLGA(PTX), c) BN-PLGA(PTX) and d) SEM image of PLGA NPs.

of the zeta potential. BN conjugation efficiency, indirectly measured by HPLC, was calculated to be > 97%. The measured diameters of the nanoparticles could be affected by shrinking producing a structure modification. It is possible that NPs become highly porous, which could contribute to the changes observed in the nanoparticle average size evaluated by SEM with respect to DLS results, although without statistically significant differences.

In terms of physicochemical properties, a significant accumulation of bombesin-grafted nanoparticles on tumor tissue is expected by two different mechanisms, the enhanced permeability and retention (EPR) effect and active targeting thorough GRP cell receptors. Then, in the neovasculature of tumor, the characteristic fenestrations of 200–780 nm would allow the extravasation of ^{177}Lu-BN-PLGA(PTX) (200 nm) in the tumoral acid microenvironment, with the consequent PTX delivery and cancer cell internalization by simple PTX diffusion due to its small molecule size and lipophilic properties (< 1000 Da). ^{177}Lu-BN-PLGA(PTX) could also be actively incorporated into the cell by different endocytic pathways attributed to the specific recognition by the GRPr [12,23,24].

3.3. Radiolabeling efficiency and radiochemical purity

Radiolabeling efficiency of the nanosystems was determined by ultracentrifugation (45%), and after purification, radiochemical purity (evaluated by ITLC) was 99 ± 1%.

3.4. Infrared spectroscopy

The PLGA nanoparticle spectrum was consistent with that previously reported [11,14]. Characteristic vibrational modes were observed, such as $(C-H)_{\upsilon}$ from the co-polymer carbon skeletal between 2942 cm^{-1} and 2918 cm^{-1}, $(C=O)_{\upsilon}$ vibration of the ester group at 1752 cm^{-1}, $(C-H)_{\delta}$ from bonds between monomeric units of lactide-glycolide (L-G: 1376 cm^{-1}), glycolide-glycolide (G-G: 1425 cm^{-1}) and lactide-lactide (L-L: 1453 cm^{-1}) and $(C-O)_{\upsilon}$, $(O-H)_{\delta}$ and $(O-H)_{\upsilon}$ as evidence of stabilization with PVA (Fig. 3c).

IR analysis of the PTX was consistent with previous reports [25]. Briefly, the spectrum showed stretching (−N−H) vibrations characterized by a broad and asymmetric band centered at 3442 cm^{-1}. The band found at 2945 cm^{-1} was assigned to (−C−H) from asymmetric and symmetric stretching vibrations. The amide I region mainly associated with a (C=O) stretching vibration was identified at 1732 cm^{-1}, whereas (C−N) stretching was found at 1274 cm^{-1}. Aromatic hydrocarbons were identified by characteristic absorption bands in the region near to 1645 cm^{-1} and 1500–1400 cm^{-1}, produced by carbon-carbon stretching vibrations in the aromatic ring. The bands in the 1250–1000 cm^{-1} region were assigned to C−H in-plane bending, and finally, C−H stretching above 3000 cm^{-1} was also identified (Fig. 3a).

The IR spectrum corresponding to paclitaxel-loaded PLGA nanoparticles (Fig. 3d) showed no difference with regard to the empty nanoparticle spectrum. These spectra did not display the characteristic intense bands from free PTX; they may have been masked by the bands produced by the polymer. The possible absence of chemical interaction between the polymer and drug may indicate a complete encapsulation of paclitaxel into the nanoparticles [26,27].

The spectra of pure Lys^{1}Lys^3(DOTA)BN (Fig. 3b) showed characteristic peaks at 3283, 1646 and 1533 cm^{-1}, corresponding to −NH stretching, C=O stretching (Amide *I*) and −CN (amide II), as previously reported [28].

BN-conjugated nanoparticles (BN-PLGA(PTX) showed the contribution of characteristic vibrations from each component. The peaks at 1666 cm^{-1} and 1536 cm^{-1} on BN-PLGA(PTX) from amide stretching vibrations makes the presence of BN in PLGA nanoparticles evident (Fig. 3e).

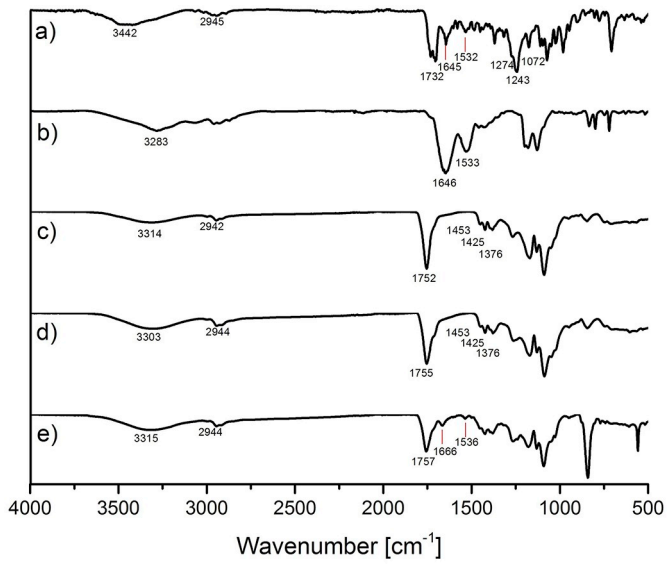

Fig. 3. Infrared spectra of a) paclitaxel, b) Lys^{1}Lys^3(DOTA)Bombesin, c) PLGA nanoparticles d) PLGA(PTX) nanoparticles and e) BN-PLGA(PTX) nanoparticles.

3.5. Encapsulation efficiency (EE) and drug loading (DL)

The efficiency of hydrophobic paclitaxel encapsulation in BN-PLGA(PTX) was calculated by subtracting the free drug measured in a filtered solution from the total amount used to prepare the nanoparticles. HPLC analysis was carried out at λ_{max} = 227 nm, using a standard curve related to the absorption and PTX concentration (6.0–300.0 μg/mL r^2 = 0.997). The efficiency of drug encapsulation was 92.8% ± 3.6, in agreement with similar reports [26,29,30]; and drug loading was 1.13 ± 0.13%. It was observed that loading capacity decreases in function of the size; thus high concentration of nanoparticles may be needed for therapeutic efficacy.

3.6. In vitro release

To evaluate the controlled release capacity of PTX from BN-PLGA(PTX), the nanosystem was evaluated in simulated physiological pH (7.4) and acidic microenvironment tumor conditions (pH 5.3). The cumulative release percentage of PTX is shown in Fig. 4.

The kinetic drug release profiles exhibited biphasic patterns with release during the first 25 h of 66.8% and 63.7% at pH 5.3 and 7.4,

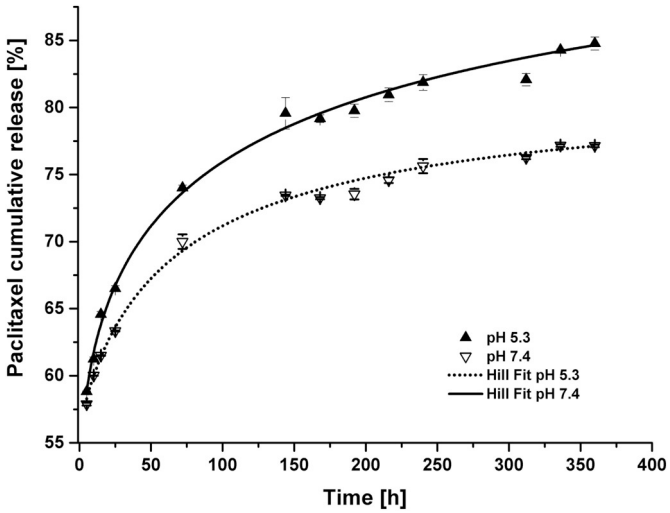

Fig. 4. *In vitro* release of PTX from paclitaxel-loaded PLGA nanoparticles in PBS (pH 5.3 and 7.4) fitted to the non-linear Hill model.

respectively, followed by a slow and continuous release during 15 days. Significant differences ($p < 0.05$) dependent on pH were observed, the maximum amount of drug release was reached at pH 5.3 (84.8%), whereas at pH 7.4 the maximum release was 77.1% of the total entrapped drug. As it is known, the higher release at pH 5.3 is attributed to the effect of hydrolysis and degradation of the polymer [31]. Therefore, paclitaxel release from BN-PLGA(PTX) in the acidic tumor microenvironment may have an improvement over anticancer drug delivery. The presented results support the proposal that loading hydrophobic molecules such as PTX on PLGA nanoparticles could enhance their accumulation on tumor tissues with the consequent decrease of the adverse effects produced by the drug.

3.7. In vitro uptake study

The therapeutic efficiency of paclitaxel-loaded PLGA depends on the nanosystem cell uptake, their intracellular distribution, and the release from internalized nanoparticles.

As previously reported, GRPr is overexpressed in several breast cancer cell lines such as MDA-MB-231 and T47D [16,17,32]. Cell uptake was evaluated comparing the behavior of ^{177}Lu-BN-PLGA(PTX) and ^{177}Lu-BN as a monomeric system. The results showed a specific uptake of ^{177}Lu-BN-PLGA(PTX) de 4.58 ± 0.42%, which was significantly reduced ($p < 0.05$) when GRP receptors of MDA-MB-231 cells were blocked by pre-incubation (10 min before treatment exposure) with free Lys^{1}Lys^{3}BN peptide (Fig. 5a). This evidence suggests that the active targeting was achieved due to the PLGA surface modification with BN.

The specific uptake of ^{177}Lu-BN was also confirmed. It was the highest uptake value observed (8.20 ± 0.49%), which was effectively diminished (1.6 ± 0.26%) when receptors were previously blocked in the presence of 5.7 μM Lys^{1}Lys^3(DOTA)-BN (10 min of pre-incubation) (Fig. 5a). While the free PTX does not require a ligand-receptor interaction to mediate endocytosis, ^{177}Lu-BN-PLGA(PTX) is introduced into the cell through several mechanisms. It has been demonstrated that nanoparticle systems conjugated to bombesin interact specifically with GRP receptors, increasing the ligand internalization by clathrin-mediated endocytosis, and thus allow a suitable delivery of paclitaxel into MDA-MB-231 cells; this enables the system to produce a higher level of toxicity [22,33].

Therefore, ^{177}Lu-BN-PLGA(PTX) nanosystems exhibited cellular uptake based on receptor-mediated endocytosis attributed to the interaction of BN with the GRP receptor. The active targeting was achieved by modifying the PLGA with BN. However, further information on the kinetics of internalization is needed to correlate the cargo delivery profile to understand the *in vitro* behavior.

3.8. Estimation of radiation-absorbed doses to the MDA-MB-231cell nucleus

Based on the uptake (radioactivity in the membrane) and internalization (radioactivity in cytoplasm) results as well as ^{177}Lu decay properties, the biokinetic models of ^{177}Lu-BN-PLGA(PTX) and ^{177}Lu-BN were obtained and the radiation absorbed doses calculated for MDA-MB-231 cells.

The total absorbed dose produced to the cell nuclei by ^{177}Lu-BN at 72 h was 0.659 Gy, 1.6 times higher than that produced by ^{177}Lu-BN-PLGA(PTX) (0.400 Gy, Table 2). All the estimated doses delivered by each treatment were lower than 1 Gy. In this regard, it is reported that a dose of 100 Gy is required to destroy cell function in non-proliferating systems, and the mean lethal dose for loss of proliferative capacity is about 2 Gy [34]. Moreover, a recent study demonstrated that the radiation-absorbed dose in the nucleus of 4.8 Gy on lymphoma cells induced DNA damage and produced an important increase in the apoptotic cell population (98%), mostly in late-stage (irreversible) apoptosis [35]. As previously mentioned, our intention during the cytotoxicity evaluation was to evaluate differences between ^{177}Lu treatments without inducing cell death, which is why doses below 2 Gy were used. However, for the study of the synergistic therapeutic effect, doses of 8 Gy were applied (Table 2).

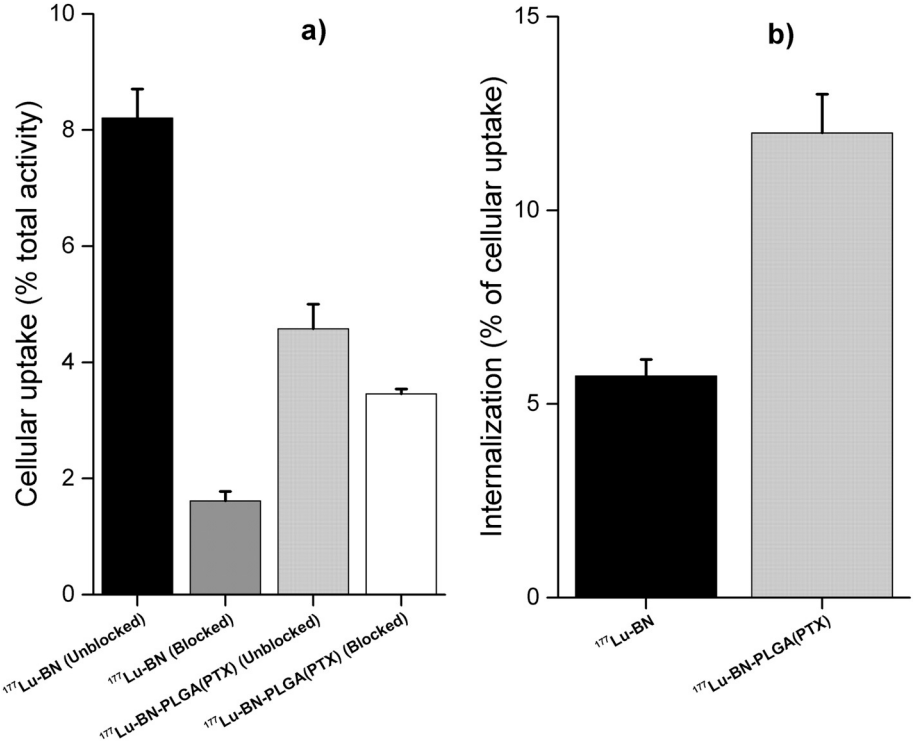

Fig. 5. a) ^{177}Lu-BN and ^{177}Lu-BN-PLGA(PTX) cellular uptake. Pre-incubated MDA-MB-231 cells with Lys^{1}Lys^3-DOTA-BN (blocked receptors) and without Lys^{1}Lys^3(DOTA)-BN pre-incubation (unblocked receptors) and b) internalization with regard to total uptake.

Table 2
Biokinetic model and radiation absorbed doses produced by 0.5 Bq/cell of ^{177}Lu-radiopharmaceuticals to the MDA-MB-231 cancer cell nuclei within 72 h.

Radiopharmaceutical cellular location	Biokinetic model $A(t)$	$N = \int_{t=0}^{t=72\,h} A(t)dt$	Dose (Gy)	Total dose to cell nuclei (Gy)
^{177}Lu-BN-PLGA(PTX)				0.400
Membrane	$A(t) = 0.089e^{-3.96t} + 3.730e^{-0.009t} + 0.780e^{-0.007t}$	8712	0.332	
Cytoplasm	$A(t) = 9.880e^{-10.004t} + 0.159e^{-0.008t} + 0.337e^{-0.008t}$	1004	0.075	
^{177}Lu-BN				0.659
Membrane	$A(t) = 0.422e^{-25.404t} + 6.25e^{-0.008t} + 1.98e^{-0.010t}$	15,912	0.594	
Cytoplasm	$A(t) = 0.439e^{-28.704t} + 0.132e^{-0.012t} + 0.337e^{-0.008t}$	904	0.065	

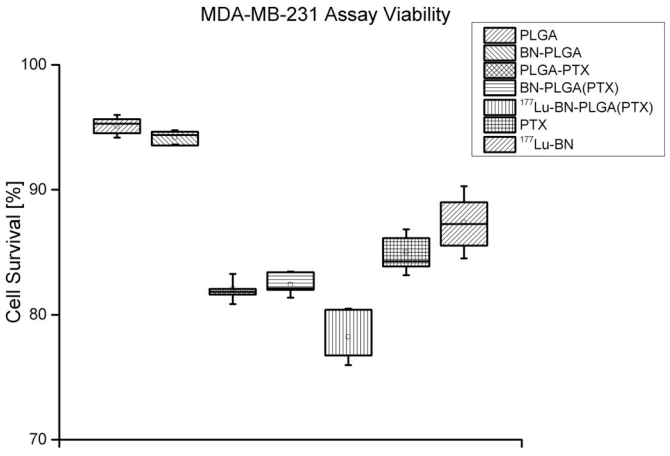

Fig. 6. Effect on cell viability after exposure of MDA-MB-231 cells to sublethal doses of paclitaxel (1.5 μM) and ^{177}Lu radiation doses (< 1 Gy) in different nanosystems.

3.9. In vitro cytotoxicity

Fig. 6 shows that ^{177}Lu-BN-PLGA(PTX) caused a significant decrease in cell viability when compared to BN-PLGA(PTX), ^{177}Lu-BN or PTX.

At 72 h of treatment, 0.40 Gy of radiation absorbed dose was deposited into the nucleus of an MDA-MB-231 cell treated with ^{177}Lu-BN-PLGA(PTX). At this time point, the viability decreased to 78.9 ± 2.61%, which was significantly different compared to BN-PLGA (94.1 ± 0.5%, $p < 0.001$), PLGA (92.2 ± 3.2%, $p < 0.001$), PTX (85.0 ± 1.8%, $p < 0.001$) and ^{177}Lu-BN (87.4 ± 3.3%, $p < 0.001$), even when in the latter, the radiation absorbed dose was 0.659 Gy (Table 2).

Since the *in vitro* binding assay demonstrated specific uptake at 45 min of treatment exposure, the uptake and consequent observed cell death without a significant difference ($p < 0.05$) for the PLGA(PTX) group (90.56 ± 7.30%), compared with BN-PLGA(PTX) (84.84 ± 2.52%), was attributed to the delivered PTX as a result of the unspecific invagination produced by the weak cooperative interactions between NPs and cells. Moreover, it was expected that the endocytic pathways having low efficiency were favored by the exposition time (72 h) for both treatments. [24,36].

After 72 h, the cell viability produced by 1.5 μM of free PTX (85.0 ± 1.8%) was significantly different ($p < 0.001$) when compared with the survival rate (78.9 ± 2.61%) produced by ^{177}Lu-BN-PLGA(PTX). At this time point, an important amount of PTX (74%) had been released, contributing to the cell toxicity (Fig. 3). These results are expected since a concentration of 15 μM of PTX is required to produce significant cell death [18]. Furthermore, the encapsulation of PTX on PLGA nanoparticles enhances the cytotoxic effect (Fig. 6).

In terms of radiosensitization, nanoparticles encapsulating chemical compounds have been proposed to enhance the response to radiation [37]. In Fig. 6, the synergistic effect between chemotherapy and radiotherapy is observed. The high decrease in viability produced by

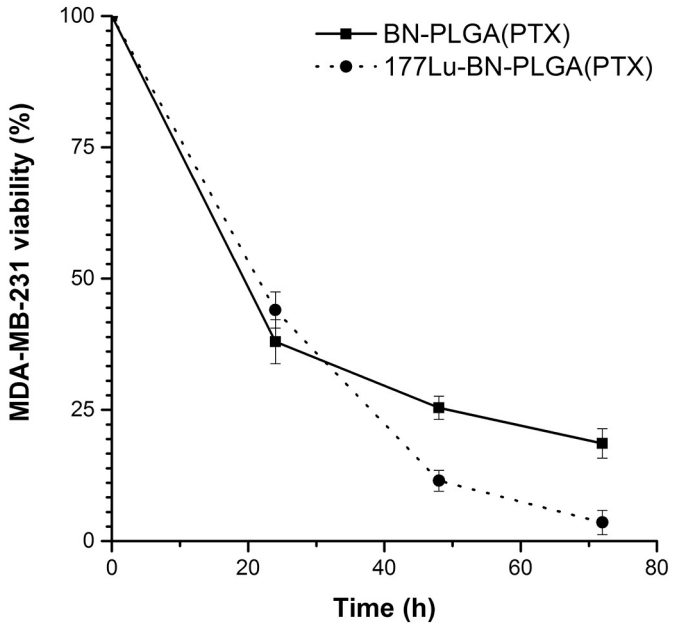

Fig. 7. Effect on MDA-MB-231cell viability after exposure to ^{177}Lu-BN-PLGA(PTX), compared to BN-PLGA(PTX). PTX = 30 μM, radiation dose = 8 Gy at 72 h.

^{177}Lu-BN-PLGA(PTX) between 24 and 48 h is mainly attributed to the radiosensitization effect produced by PTX.

The synergistic effect of chemotherapy and radiotherapy produced by the ^{177}Lu-BN-PLGA(PTX) nanosystem was evident when doses of PTX = 30 μM and radiation-absorbed doses of 8 Gy were used. As can be observed in Fig. 7, the greater cytotoxic effect for the radiolabeled nanosystem was observed between 24 and 72 h (highest slope) given that, at this time, a significant PTX and radiation dose delivery had occurred.

3.10. Hemocompatibility

The non-hemolytic behavior of the ^{177}Lu-BN-PLGA(PTX) supports its suitability for intravenous administration (0.97 ± 0.05%). The systems can be classified as non-hemolytic materials, based on the hemolysis value being lower than 2% [38].

3.11. In vivo studies

Fig. 8a shows a representative SPECT image of a mouse with an MDA-MB-231 pulmonary tumor model. The tumor-to-blood ratio reveals suitable contrast, with a significant accumulation of ^{177}Lu-BN-PLGA(PTX) nanomedicine in tumor tissue after 72 h of injection with a standard uptake value (SUV) of 3. The *ex vivo* biodistribution results of ^{177}Lu-BN-PLGA(PTX) also showed a high tumor uptake in MDA-MB-231 lesions (Fig. 8b). However, future studies are required to obtain a complete ^{177}Lu-BN-PLGA(PTX) biokinetic profile for the *in vivo*

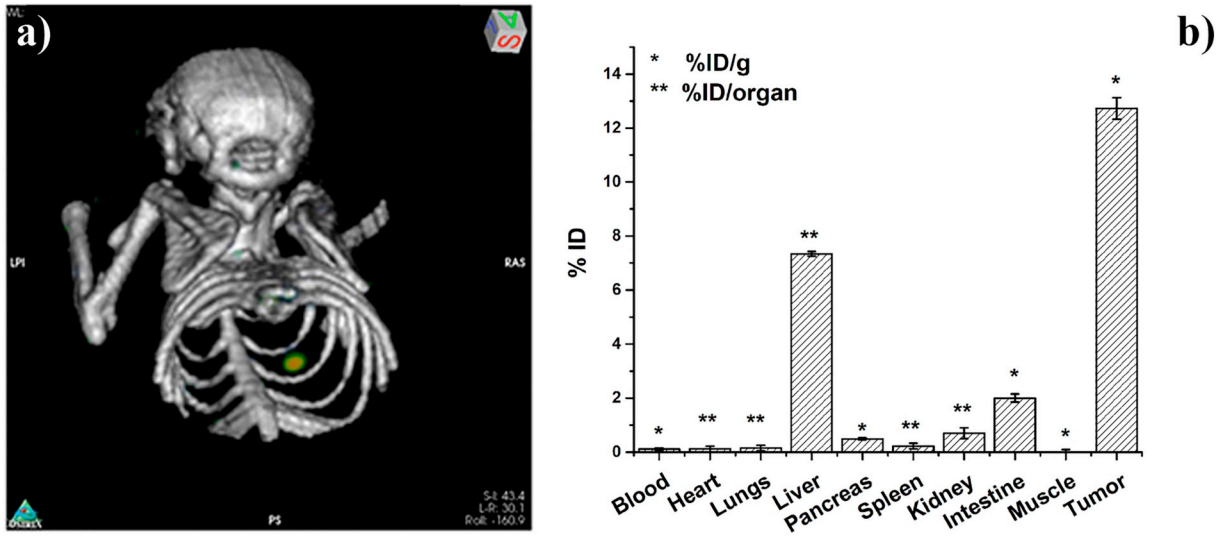

Fig. 8. a) Micro SPECT-CT image (72 h) in athymic mice with pulmonary tumor model (MDA-MB-231 cells) and b) biodistribution of ^{177}Lu-BN-PLGA(PTX) in athymic mice with subcutaneous tumor model (MDA-MB-231 cells), 72 h post-injection.

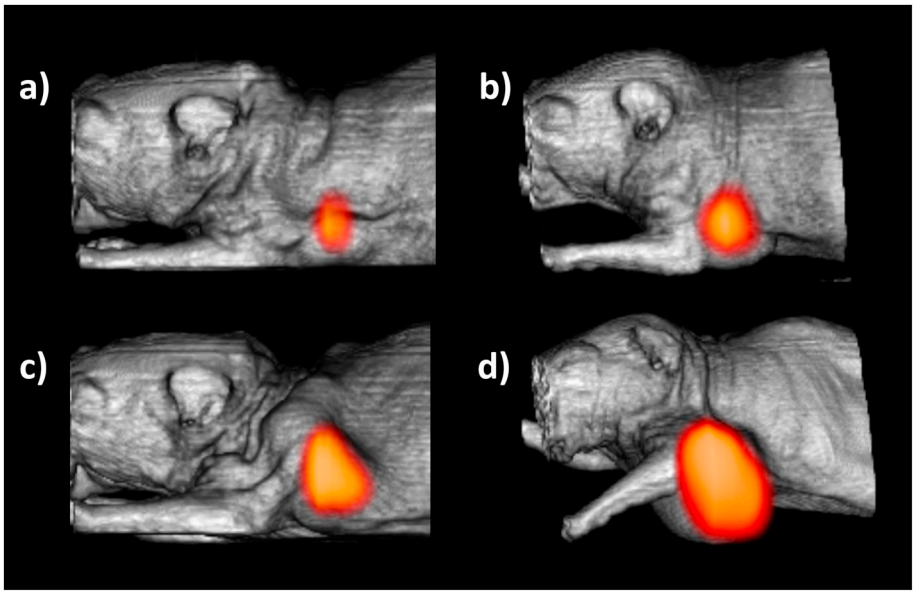

Fig. 9. Micro PET-CT images of a) ^{177}Lu-BN-PLGA(PTX), b) ^{177}Lu-BN-PLGA, c) PLGA(PTX) and d) PLGA as the control group, after 8 days post-administration of 3 MBq of ^{177}Lu-BN-PLGA(PTX), 3 MBq of ^{177}Lu-BN-PLGA and μg of PLGA(PTX) and PLGA. The heart FDG uptake was subtracted from the image to visualize the tumor uptake.

absorbed dose assessment and for the evaluation of its therapeutic efficacy in different breast cancer models.

Since the micro-PET/CT imaging at the end of the *in vivo* studies showed a tumor volume for the mice control group of 1.83 ± 0.54 cm^3, the combination of targeted radiotherapy (provided by ^{177}Lu-BN) and chemotherapy (provided by PTX) resulted in the highest inhibition of breast tumor growth for the mice administered with ^{177}Lu-BN-PLGA(PTX), which reached the lowest tumor proliferation (0.136 ± 0.04 cm^3). The group exposed to ^{177}Lu-BN-PLGA produced a final tumor of 0.654 ± 0.202 cm^3 and the PLGA(PTX) group produced a tumoral volume of 0.216 ± 0.072 cm^3. Therefore, the response to treatment was in this order: ^{177}Lu-BN-PLGA(PTX) > PLGA(PTX) > ^{177}Lu-BN-PLGA > PLGA (control).

The SUV data, related directly to the metabolic activity, were 42.43 ± 5.54, 24.31 ± 4.51, 14.74 ± 2.92 and 8.10 ± 1.06 for the control group, ^{177}Lu-BN-PLGA, PLGA(PTX), ^{177}Lu-BN-PLGA(PTX), respectively. Even though the average radiation-absorbed dose of ^{177}Lu-BN-PLGA(PTX) and ^{177}Lu-BN-PLGA delivered to the tumor was the same (36.9 ± 7.01 Gy), and this dose corresponds to that usually applied in radiotherapy treatments to breast cancer patients, the ^{177}Lu-BN-PLGA(PTX) conjugated showed the lowest tumoral metabolic activity (lowest SUV) and almost complete inhibition of the tumor progression (lowest tumoral volume). These results corroborate the synergistic effect between radiation therapy and chemotherapy in a single nanosystem (Fig. 9).

4. Conclusions

^{177}Lu-BN-PLGA(PTX) nanoparticles are suitable systems for the bimodal therapy of breast cancer due to the synergistic effect on cell viability of the ^{177}Lu radiation dose delivery and the controlled release of paclitaxel. The radiolabeling of BN-PLGA(PTX) with Lu-177 allows for the acquisition of GRPr overexpression images in breast cancer tumors, making the monitoring of disease progression possible. Further studies are needed to determine the therapeutic efficacy of ^{177}Lu-BN-PLGA(PTX) in different breast cancer preclinical models.

Funding statement

This study was supported by the International Atomic Energy

Agency (CRP—F22064, contract No. 18358) and was carried out as part of the activities of the "Laboratorio Nacional de Investigación y Desarrollo de Radiofármacos, CONACyT".

Declaration of competing interest

The authors declare that there are no conflicts of interest regarding the publication of this paper.

Acknowledgments

The authors thank Jorge E. Pérez del Prado for his support during SEM analyses. This study was partially supported by the National Council of Science and Technology (CONACyT-CB-A1S38087) and the International Atomic Energy Agency (CRP-F22064, Contract 18358). It was carried out as part of the activities of the "Laboratorio Nacional de Investigación y Desarrollo de Radiofármacos, CONACyT.

References

[1] S. Mann, A. Dufour, J. Glass, R. De Rose, S. Kent, G. Such, A. Johnston, Tuning the properties of pH responsive nanoparticles to control cellular interactions in vitro and ex vivo, Polym. Chem. 7 (38) (2016) 6015–6024.
[2] A. Srivastava, T. Yadav, S. Sharma, A. Nayak, A.A. Kumari, N. Mishra, Polymers in drug delivery, J Biosci Med 4 (01) (2015) 69.
[3] D. Kapoor, A. Bhatia, R. Kaur, R. Sharma, G. Kaur, S. Dhawan, PLGA: a unique polymer for drug delivery, Ther. Deliv. 6 (1) (2015) 41–58.
[4] S.-S. Feng, L. Mu, K.Y. Win, G. Huang, Nanoparticles of biodegradable polymers for clinical administration of paclitaxel, Curr. Med. Chem. 11 (4) (2004) 413–424.
[5] C. de Aguiar Ferreira, L.L. Fuscaldi, D.M. Townsend, D. Rubello, A.L.B. de Barros, Radiolabeled bombesin derivatives for preclinical oncological imaging, Biomed. Pharmacother. 87 (2017) 58–72.
[6] P. Fernandez, M. Debled, E. Hindié, Expression of gastrin-releasing peptide receptor in breast cancer and its association with pathologic, biologic, and clinical parameters: a study of 1,432 primary tumors, J. Nucl. Med. 58 (2017) 1401–1407.
[7] T. Maina, B.A. Nock, H. Kulkarni, A. Singh, R.P. Baum, Theranostic prospects of gastrin-releasing peptide receptor–radioantagonists in oncology, PET clinics 12 (3) (2017) 297–309.
[8] B.B.S. Cerqueira, A. Lasham, A.N. Shelling, R. Al-Kassas, Development of biodegradable PLGA nanoparticles surface engineered with hyaluronic acid for targeted delivery of paclitaxel to triple negative breast cancer cells, Mater. Sci. Eng. C. 76 (2017) 593–600.
[9] H. Mendoza-Nava, G. Ferro-Flores, F.d.M. Ramírez, B. Ocampo-García, C. Santos-Cuevas, E. Azorín-Vega, N. Jiménez-Mancilla, M. Luna-Gutiérrez, K. Isaac-Olivé, Fluorescent, plasmonic, and radiotherapeutic properties of the ^{177}Lu–dendrimer-AuNP–folate–bombesin nanoprobe located inside cancer cells, Mol. Imaging 16 (2017) (1536012117704768).
[10] N. Jiménez-Mancilla, G. Ferro-Flores, C. Santos-Cuevas, B. Ocampo-García, M. Luna-Gutiérrez, E. Azorín-Vega, K. Isaac-Olivé, M. Camacho-López, E. Torres-García, Multifunctional targeted therapy system based on 99mTc/^{177}Lu-labeled gold nanoparticles-Tat (49–57)-Lys3-bombesin internalized in nuclei of prostate cancer cells, J. Label. Compd. Radiopharm. 56 (13) (2013) 663–671.
[11] H. Kulhari, D. Pooja, S. Shrivastava, V. Naidu, R. Sistla, Peptide conjugated polymeric nanoparticles as a carrier for targeted delivery of docetaxel, Colloids Surf. B 117 (2014) 166–173.
[12] H. Kulhari, D. Pooja, M.K. Singh, M. Kuncha, D.J. Adams, R. Sistla, Bombesin-conjugated nanoparticles improve the cytotoxic efficacy of docetaxel against gastrin-releasing but androgen-independent prostate cancer, Nanomedicine 10 (18) (2015) 2847–2859.
[13] L. Bodei, M. Ferrari, A. Nunn, J. Llull, M. Cremonesi, L. Martano, G. Laurora, E. Scardino, S. Tiberini, G. Bufi, Lu-177-AMBA bombesin analogue in hormone refractory prostate cancer patients: a phase I escalation study with single-cycle administrations, European Journal of Nuclear Medicine and Molecular Imaging (2007) S221 SPRINGER 233 Spring Street, New York, NY 10013 USA.
[14] L. Jaimes-Aguirre, E. Morales-Avila, B.E. Ocampo-García, L.A. Medina, G. López-Téllez, B.V. Gibbens-Bandala, V. Izquierdo-Sánchez, Biodegradable poly(D,L-lactide-co-glycolide)/poly(L-γ-glutamic acid) nanoparticles conjugated to folic acid for targeted delivery of doxorubicin, Mater. Sci. Eng. C Mater. Biol. Appl. 76 (2017) 743–751.
[15] B. Gibbens-Bandala, B. Ocampo-García, G. Ferro-Flores, E. Morales-Avila, A. Ancira-Cortez, L. Jaimes-Aguirre, Multimeric system of RGD-grafted PMMA-nanoparticles as a targeted drug-delivery system for paclitaxel, Curr. Pharm. Des. 23 (23) (2017) 3415–3422.
[16] M. Miyazaki, N. Lamharzi, A.V. Schally, G. Halmos, K. Szepeshazi, K. Groot, R.Z. Cai, Inhibition of growth of MDA-MB-231 human breast cancer xenografts in nude mice by bombesin/gastrin-releasing peptide (GRP) antagonists RC-3940-II and RC-3095, Eur. J. Cancer 34 (5) (1998) 710–717.
[17] C. Chao, K. Ives, H.L. Hellmich, C.M. Townsend, M.R. Hellmich, Gastrin-releasing peptide receptor in breast cancer mediates cellular migration and interleukin-8 expression, J. Surg. Res. 156 (1) (2009) 26–31.
[18] N. Hasima, L.I.L. Aun, M.N. Azmi, A.N. Aziz, E. Thirthagiri, H. Ibrahim, K. Awang, 1′ S-1′-acetoxyeugenol acetate: a new chemotherapeutic natural compound against MCF-7 human breast cancer cells, Phytomedicine 17 (12) (2010) 935–939.
[19] S.M. Goddu, T.F. Budinger, MIRD cellular S. values: self-absorbed dose per unit cumulated activity for select radionuclides and monoenergetic electron and alpha particle emitters incorporated into different cell compartments, Society of Nuclear Medicine 1 (1997) 120.
[20] A. Escudero-Castellanos, B.E. Ocampo-García, M.V. Domínguez-García, J. Flores-Estrada, M.V. Flores-Merino, Hydrogels based on poly(ethylene glycol) as scaffolds for tissue engineering application: biocompatibility assessment and effect of the sterilization process, J Mater Sci Mater Med 27 (12) (2016) 176.
[21] A. Vilchis-Juárez, G. Ferro-Flores, C. Santos-Cuevas, E. Morales-Avila, B. Ocampo-García, L. Díaz-Nieto, M. Luna-Gutiérrez, N. Jiménez-Mancilla, M. Pedraza-López, L. Gómez-Oliván, Molecular targeting radiotherapy with cyclo-RGDFK (C) peptides conjugated to ^{177}Lu-labeled gold nanoparticles in tumor-bearing mice, J. Biomed. Nanotechnol. 10 (3) (2014) 393–404.
[22] C. Sengel-Turk, C. Hascicek, A. Dogan, G. Esendagli, D. Guc, N. Gonul, Surface modification and evaluation of PLGA nanoparticles: the effects on cellular uptake and cell proliferation on the HT-29 cell line, J Drug Deliv Sci Technol 24 (2) (2014) 166–172.
[23] M. Gaumet, A. Vargas, R. Gurny, F. Delie, Nanoparticles for drug delivery: the need for precision in reporting particle size parameters, Eur. J. Pharm. Biopharm. 69 (1) (2008) 1–9.
[24] J.s. Mosquera, I. García, L.M. Liz-Marzán, Cellular uptake of nanoparticles versus small molecules: a matter of size, Acc. Chem. Res. 51 (9) (2018) 2305–2313.
[25] J.G. Hiremath, N.S. Khamar, S.G. Palavalli, C.G. Rudani, R. Aitha, P. Mura, Paclitaxel loaded carrier based biodegradable polymeric implants: preparation and in vitro characterization, Saudi Pharm J 21 (1) (2013) 85–91.
[26] K.F. Martins, A.D. Messias, F.L. Leite, E.A. Duek, Preparation and characterization of paclitaxel-loaded PLDLA microspheres, Mater. Res. 17 (3) (2014) 650–656.
[27] F. Yerlikaya, A. Ozgen, I. Vural, O. Guven, E. Karaagaoglu, M.A. Khan, Y. Capan, Development and evaluation of paclitaxel nanoparticles using a quality-by-design approach, J. Pharm. Sci. 102 (10) (2013) 3748–3761.
[28] L. Aranda-Lara, G. Ferro-Flores, E. Azorín-Vega, F. de María Ramírez, N. Jiménez-Mancilla, B. Ocampo-García, C. Santos-Cuevas, K. Isaac-Olivé, Synthesis and evaluation of Lys 1 (α, γ-folate) Lys 3 (177 Lu-DOTA)-Bombesin (1-14) as a potential theranostic radiopharmaceutical for breast cancer, Appl. Radiat. Isot. 107 (2016) 214–219.
[29] R.K. Averineni, G.V. Shavi, A.K. Gurram, P.B. Deshpande, K. Arumugam, N. Maliyakkal, S.R. Meka, U. Nayanabhirama, PLGA 50: 50 nanoparticles of paclitaxel: development, in vitro anti-tumor activity in BT-549 cells and in vivo evaluation, Bull. Mater. Sci. 35 (3) (2012) 319–326.
[30] C. Fonseca, S. Simões, R. Gaspar, Paclitaxel-loaded PLGA nanoparticles: preparation, physicochemical characterization and in vitro anti-tumoral activity, J. Control. Release 83 (2) (2002) 273–286.
[31] H. Maleki, F. Dorkoosh, M. Adabi, M. Khosravani, H. Arzani, M. Kamali, Methotrexate-loaded plga nanoparticles: preparation, characterization and their cytotoxicity effect on human glioblastoma U87MG cells, Int J Med Nano Res 4 (1) (2017) 020.
[32] S. Giacchetti, C. Gauvillé, P.D. Crémoux, L. Bertin, P. Berthon, J.P. Abita, F. Cuttitta, F. Calvo, Characterization, in some human breast cancer cell lines, of gastrin-releasing peptide-like receptors which are absent in normal breast epithelial cells, Int. J. Cancer 46 (2) (1990) 293–298.
[33] D. Suresh, A. Zambre, N. Chanda, T. Hoffman, J. Smith, Bombesin peptide conjugated gold nanocages internalize via clathrin mediated endocytosis, Bioconjug. Chem. 25 (2014) 1565–1579.
[34] E.J. Hall, A.J. Giaccia, Radiobiology for the Radiologist, Lippincott Williams & Wilkins, Philadelphia, 2006.
[35] E. Azorín-Vega, E. Rojas-Calderón, B. Martínez-Ventura, J. Ramos-Bernal, L. Serrano-Espinoza, N. Jiménez-Mancilla, D. Ordaz-Rosado, G. Ferro-Flores, Assessment of cell death mechanisms triggered by ^{177}Lu-anti-CD20 in lymphoma cells, Appl. Radiat. Isot. 138 (2018) 73–77.
[36] P. Decuzzi, M. Ferrari, The role of specific and non-specific interactions in receptor-mediated endocytosis of nanoparticles, Biomaterials 28 (18) (2007) 2915–2922.
[37] J.W. Bergs, M.G. Wacker, S. Hehlgans, A. Piiper, G. Multhoff, C. Roedel, F. Roedel, The role of recent nanotechnology in enhancing the efficacy of radiation therapy, Biochim. Biophys. Acta 1856 (1) (2015) 130–143.
[38] A. Escudero-Castellanos, B.E. Ocampo-García, G. Ferro-Flores, K. Isaac-Olivé, C.L. Santos-Cuevas, A. Olmos-Ortiz, J. García-Quiroz, R. García-Becerra, L. Díaz, Preparation and in vitro evaluation of ^{177}Lu-iPSMA-RGD as a new heterobivalent radiopharmaceutical, J. Radioanal. Nucl. Chem. 314 (3) (2017) 2201–2207.